ADVANCED MATERIALS INTERFACES
www.advmatinterfaces.de

A New Approach to Polymorphism in Molecular Crystals: Substrate-Mediated Structures Revealed by Lattice Phonon Dynamics

Tommaso Salzillo and Aldo Brillante**

The issue of polymorphism in molecular crystals is discussed, taking into account the substrate-mediated structures, that is, structures grown at the interface of different substrates. Bulk and thin films of a compound both share the potentiality to display different crystal forms. However, unlike bulk polymorphs, whose structures are determined by their different molecular packing, thin film structures depend very much on the molecular organization of the organic layers on the substrate, which may, or may not, lead to an ordered structure, depending on the nature of the interface and on the growth conditions. Based on large part in some of the authors' recent works, these thin film structures are classified as distorted bulk, substrate-selected and substrate-stabilized polymorphs, with some subtle differences which may yield a polymorph to belong not exclusively to a single one of these categories. Some experiments are then focused upon, involving charge transport at the interface, as well as how far the effect of the surface goes. Furthermore, the authors comment on how the surface-mediated structures evolve to the single crystal phase in the cases of pentacene and α-sexithiophene. Finally, the transition from a 3- to a 2D regime of growth is shortly discussed in terms of low-dimensional disorder.

1. Introduction

Polymorphism is an evergreen subject, which has been, and still is, a hot scientific and technical issue in crystallography and materials science. The book of Joel Bernstein[1] represents the most comprehensive account of this phenomenon for molecular crystals. In addition, a number of good reviews has appeared in the literature, spanning a number of fields, such as pharmaceutics,[2] functional materials and their technological applications,[3] organic electronics[4,5] and crystal engineering.[6,7] The experimental search for polymorph screening is often assisted by computational studies on crystal structure predictions.[8] Lastly, a subtle perspective of Bernstein cleared up a final revision of the terminology and of the nomenclature of multiple crystal forms.[9]

In more recent years a new approach to polymorphism has taken momentum in the search of new crystal structures of organic materials, the so-called thin film structures or substrate-induced polymorphs (SIP), meaning a phase grown in the vicinity of a substrate with a distinct structure from those of the bulk.[10]

An earlier discussion on the subject was held in a dedicated workshop about fifteen years ago.[11] At that time the discussion was mostly focused on organic semiconductors such as pentacene and perylene diimide derivatives. Since the majority of the thin film structures showed crystal parameters not very dissimilar from those of the corresponding parent bulk forms, these structures were indicated as "distorted-bulk," where the term "distorted" was ascribed to the perturbation of the substrate on the molecular layers. Approximately ten years later,[12] a new grammar on substrate-induced structures was established. The growth at the interface of a variety of different substrates led to the definition of the general class of surface-mediated structures, portraying more detailed definitions such as "surface-induced" and "surface-selected" polymorphs, with the former indicating a bulk-distorted form and the latter being a new genuine structure with no association to any crystal phase of the bulk. This is the nomenclature that we shall initially follow in the present survey, with some new hints on additional cases that will be encountered, such as substrate-stabilized polymorphs, as detailed further on.

Certainly, the starting point of surface-mediated polymorphs cannot be separated by the exhaustive review on SIP as discussed in Jones et al.[10] In that paper, examples of sixteen molecules were given, for which thin film polymorphs had been observed on solid substrates, showing new structures with respect to the previously known single crystals polymorphs. The impact of polymorphism on the material properties was mostly addressed on organic electronics, because every structure has its own mobility with relevant consequences on the efficiency of the device. Besides, it is well

T. Salzillo, A. Brillante
Department of Industrial Chemistry "Toso Montanari"
and INSTM-Udr Bologna
University of Bologna
Viale del Risorgimento, 4, Bologna 40136, Italy
E-mail: tommaso.salzillo@unibo.it; aldo.brillante@unibo.it

The ORCID identification number(s) for the author(s) of this article can be found under https://doi.org/10.1002/admi.202200815.

DOI: 10.1002/admi.202200815

documented that charge transport of the organic active semiconducting layers at the interface is dominated by the very first few layers that grow in contact with the substrate, irrespective of the thickness of the molecular coverage.[13–16] Therefore, designing the interface is a core problem in thin film technology, whose capability of controlling and engineering the molecular layers of a material on a substrate may certainly lead to design the optimal physical properties for each specific application.[17]

Bulk and thin films of a compound both share the potential to display different crystal forms. However, unlike bulk polymorphs, whose structures are determined by their different molecular packing, thin film structures depend very much on the molecular organization of the organic layers on the surface, which may, or may not, lead to an ordered structure, depending on the nature of the interface and on the growth conditions. The nature of the substrate is thus crucial, because it can act as a template for epitaxial deposition, eventually leading to real new structures,[18,19] or, under other conditions, may stabilize crystal forms otherwise metastable.[20,21]

The search for new polymorphs by epitaxial growth was also studied in a following paper from the Resel Group.[22] Phase identification was performed for epitaxially grown molecular crystals by grazing incidence X-ray diffraction (GIXRD)[23] and new structures of a number of conjugated molecules were determined. Nucleation and growth of a specific structure strictly depends on the balanced interactions of the organic adsorbate with the substrate.[24,25]

Given this situation, we believe it may be helpful to provide a classification of substrate-mediated structures, in the attempt to single out distinct categories of thin film polymorphs. By no way do we mean to present an exhaustive report on the subject, we just point out a series of examples useful to advance the discussion.

The last remark is on the experimental method used to track polymorphs on substrates. Undoubtedly, structural techniques, like X-ray diffraction (XRD) or GIXRD[23] as well as morphological investigations like, for instance, atomic force microscopy (AFM), are traditionally recognized as the techniques of choice for crystal structure determination of bulk and thin film structures. However, in this short review we want to show how the use of lattice phonon dynamics, otherwise indicated as THz, or low wavenumber, Raman scattering,[26] is a fast and clever technique for polymorph recognition on surfaces.[27] Lattice phonons, probing the intermolecular interactions, are very sensitive to even slight modifications in the molecular packing, not only in the bulk crystal, but also in thin films. Besides, this non-destructive technique can be used in situ and in the confocal configuration, yielding a reliable recognition of crystal domains of different phases (phase mixing) with a spatial resolution below one micrometer, up to trace a map of the phase distribution in each specimen.[28] In all the experiments reported in the following sections we shall show how this technique has proven to be more than simply complementary to XRD and GIXRD investigations.

The experimental method based on confocal micro-Raman spectroscopy is described in the referenced papers. For a more detailed report see Brillante et al.[29]

2. Substrate-Mediated Structures

We start by defining three main categories of SIPs, that is, structures grown on a substrate: substrate-induced or bulk distorted, surface-selected and surface-stabilized polymorphs, with sometimes subtle differences which can yield a polymorph to belong not completely to a single one of these categories.

2.1. Substrate-Induced Polymorphs

The first class of compounds refers to the classical examples of polymorphs of the early organic semiconductors such as pentacene and perylene-diimide (PDI) derivatives. These structures are often not much too different in packing and density with respect to the corresponding bulk polymorphs. For this reason, they are sometimes indicated as "distorted bulk structures." These structures, by further deposition, end up invariably to a 3D growth which leads to a known bulk polymorph.

2.1.1. Pentacene

A considerable number of papers have described the state of the art of the structures and of the transport properties of pentacene. We refer to a review that exhaustively discuss growth and morphology of its thin films.[30] Here we simply summarize the structural data of the polymorphs of pentacene and of the immediate spectroscopic recognition of each phase. Two bulk polymorphs have been found as single crystals, and are called low-temperature (LT) and high-temperature (HT) phase, according to the temperature of growth.[31–34] They are both triclinic, very close in density and molecular arrangement, which shows up in a herringbone fashion. The main difference is the inter-planar distance of the *ab* planes, identified as $d = 14.4$ Å and $d = 14.1$ Å for HT and LT, respectively. The third polymorph is a thin film (TF) structure on amorphous silica substrates, with $d = 15.4$ Å, definitely assessed in subsequent structural works,[35–37] which show the long pentacene molecular axis making a slight tilt angle perpendicular to the silica surface. A structure of films deposited on NaCl has also been found.[38] Finally, the structure of a single layer, with molecules standing perpendicular to the substrate, was reported.[39,40]

Figure 1 shows how the polymorphs of pentacene can be easily recognized by their lattice phonon Raman spectra, as widely reported in the past.[41] The figure reports data of the lattice phonons and of the lowest wavenumber internal modes (a), and a selected spectral range with the C—H bending modes (b), showing that for pentacene this intramolecular region can also be diagnostic for phase recognition.

First of all, a note should be dedicated to the 1 ML Raman spectra. Though its intensity is favored by the resonance excitation conditions ($\lambda = 752.5$ nm), we are not aware of any Raman spectrum of a single layer of a molecular crystal (nominal thickness 1.5 nm) with such a signal to noise ratio. The phonon structure, though ill-defined, confirms that 1 ML of pentacene is already crystalline, with its own structure, as found by GIXRD.[39,40]

A second consideration concerns with the so called thin film (TF) phase grown on a SiO_x substrate. It is now well established that on increasing coverage the TF phase ends up to the HT phase,[10,42–45] following the Ostwald rule.[46] According

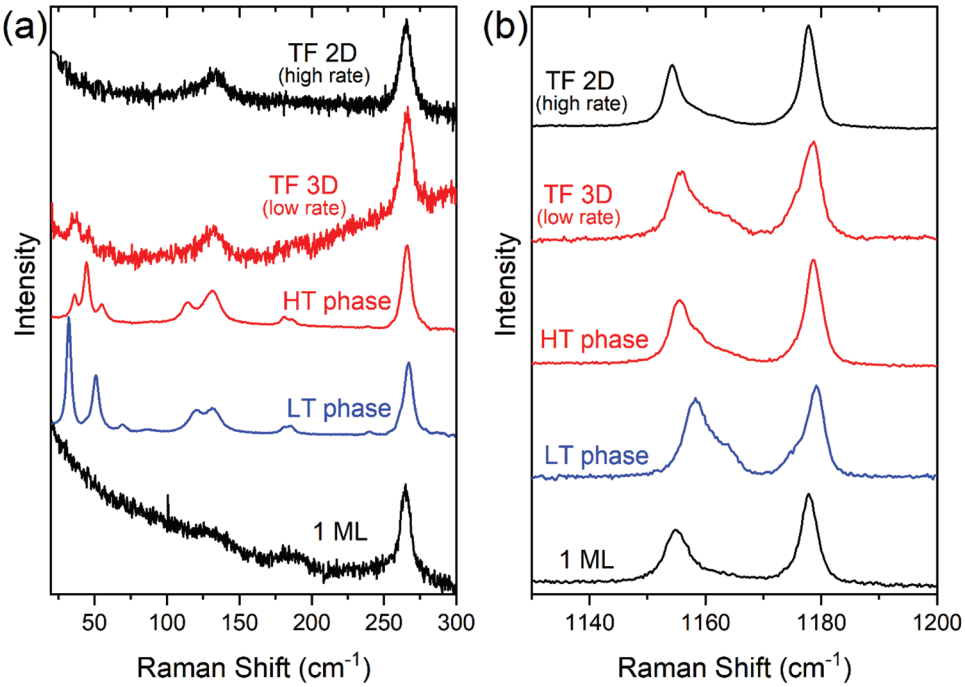

Figure 1. a) Lattice phonon spectra with the lowest wavenumber intramolecular modes and b) the C—H bending region of the bulk (LT and HT) and thin film (TF) phases, at two deposition rates, of pentacene on SiO_x. For their discussion see text. The 1 ML phase is at the bottom of both figures.

to our previous studies, this phase change occurs from about 30–50 ML,[47,48] yielding the hint that a pentacene film of 50 nm, or more, has already the bulk crystalline structure, as will be further discussed later. We have observed that the same transition can be reached by thermal annealing of the film. Increasing temperature and pressure were instead used for the transformation of the two bulk phases, LT to HT[34] and HT to LT,[49] respectively.

The fact that these structural changes can be easily monitored with lattice phonon spectra is a strong indication of how powerful THz Raman scattering can be for structure recognition, both at the bulk and SIP level. Therefore, techniques like XRD, GIXRD, THz Raman, and THz IR should all together be looked at as a body of complementary tools in studying structural changes of materials.

Finally, attention should be taken at the growing conditions of the films because the rate of growth strongly affects the outcome of the structural and charge mobility properties. Figure 1 shows (upper spectra) that high and low rate regimes, typically 2 and 0.13 nm min^{-1}, respectively, produce different spectral profiles in both the phonon and the intra-molecular regions. This depends on the effect that the growth parameters produce on the morphology of the film.[47] In fact, the architecture of the film strongly influences the transport properties of the semiconducting layer, as revealed by the effect of film crystallinity and morphology on charge carrier mobility in thin film transistors of pentacene, where it was shown that a good hole mobility could be obtained once the film was deposited at high rate.[50] This observation is fully consistent with the idea that at high rate we have a 2D growth regime,[47] with a corresponding poor interlayer correlation perpendicular to the dielectric interface. Besides, in our conditions of pentacene growth,[47] high rates yield 2D nucleation, leading to a quasi-layer-by-layer growth, forming continuous films, more suitable for charge transport.[14,50,51] On the contrary, low deposition rates yield a 3D growth, leading to ill-connected grains.[50]

These findings have their counterpart in the two upper spectra of Figure 1a, where the TF spectrum at low rate exactly matches that of the HT bulk phase, and is therefore labelled 3D. This is also confirmed by the intra-molecular spectra of Figure 1b. On the contrary it seems quite sensible that the disorder introduced in the layer-by-layer growth at the higher rate produces a "vertical" loss of correlation among the various MLs, sufficient to disrupt the phase matching in the direction perpendicular to the substrate. Spectroscopically, this produces the loss of the highly dispersed lowest wavenumber phonons.[26,47] As a consequence, the 2D structure growing at the interface produces strong effects on the mobility of the active layers, increasing the efficiency of the organic semiconductor.[50] These considerations definitely open the route to a renewed interest on the polymorphism beyond the bulk crystals. This new approach of the organic structures at the interfaces (SIP) obviously requires more investigations if we want to further improve the knowledge on the transport and structural properties of organic semiconductors.

In conclusion, from the point of view of structure recognition by means of micro-Raman spectroscopy, Figure 1 shows that at high deposition rate the outcome is the TF (2D) phase, whereas at low rate the resulting structure is that of a TF (3D) phase, matching the HT bulk polymorph. When the structural characterization reveals the coexistence of two phases, such as the HT single-crystal phase and the metastable TF phase,[42,52,53] the micro-Raman technique can be used to monitor the presence of the concomitant phases in domains at a micrometric

scale, once used in its confocal configuration.[28] This point is particularly relevant in organic semiconductors which show more polymorphs, because phase mixing constitutes an intrinsic source of disorder with detrimental effects on charge transport, and other key properties of the material.[54,55]

2.1.2. Tetracene

There are close similarities between structures and molecular arrangements of tetracene and pentacene. Like the latter, tetracene shows two polymorphs, both triclinic, one (HT) at room temperature[31,32] and the second (LT) stable at low temperature (below 140 K)[56,57] and at high pressure (above 1 GPa).[57] The corresponding lattice phonon spectra of both phases are shown in **Figure 2**a.

More important for our purposes is the structure of a thin film of 20 nm, determined by GIXRD.[58] This SIP followed a previous investigation on its coexistence with the bulk crystal, where only the parameters of the unit cell were given.[59] By looking at the unit cell of the TF structure it is evident how close the crystal parameters are when compared to those of the bulk, the two volumes differing of only 0.5%.[58] We therefore definitely classify the SIP structure of tetracene in the category of the distorted bulk polymorphs. In Figure 2b the orientation of tetracene molecules in the bulk and thin film phases is shown, whereas Figure 2c shows the X-ray reflectivity curve of a 20 nm thick tetracene film consisting of pairs of (001) reflections, an indication of the coexistence of the thin film and bulk phases.[58] We remark that this coexistence is similar to that discussed for pentacene in the previous section.

A further point linking tetracene and pentacene is related to the nucleation of the TF polymorph and to its strong relationship with the deposition rate during its growth. At low rate a 3D growth is observed, shaping the structure of the HT bulk phase, whereas increasing the rate leads to a 2D regime,[59] again in full agreement with what previously described for pentacene.[47] Experiments on lattice phonons of films grown in different conditions are encouraged to further support this hypothesis.

2.1.3. Perylene Diimide (PDI) Derivatives

Perylene diimide (PDI) derivatives represent another historical class of materials with high electron mobility, which makes them important n-type semiconductors useful for optoelectronic applications.[60–63] For some of these derivatives a number of surface-mediated structures on various substrates were reported[64,65] and many of them showed a structure very similar to the corresponding bulk phases, implying that they should be considered as distorted bulk structures, like the previously reported acenes.

Two compounds worth to mention are 3,4,9,10-perylenetetracarboxylic dianhydride (PTCDA) and *N,N′*-dimethyl 3,4,9,10-perylenetetracarboxylic diimide (DiMe-PTCDI). The molecular structures of these two molecules are quite similar and their properties have been extensively studied by Zahn.[61] The unit cells of PTCDA (two polymorphic forms[60]) and DiMe-PTCDI[66] bulk phases are both monoclinic, with a herringbone packing in the (102) planes. These two compounds were evaporated on a variety of substrates,[60] yielding thin films, whose structures showed only small deviations when compared with those of the single crystals.

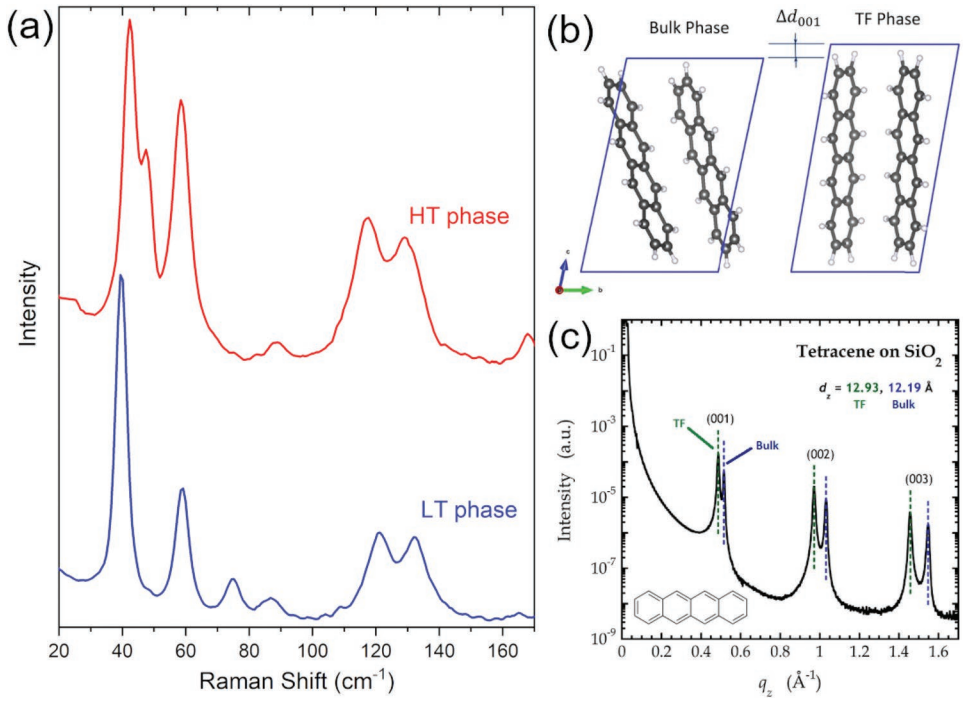

Figure 2. a) Lattice phonon Raman spectra of HT (room T, P) and LT (low T, high P) polymorphs of tetracene. b) Molecular orientations in the unit cells of the bulk and thin film phases. Reproduced with permission.[58] Copyright 2018, AIP Publishing. c) X-ray reflectivity spectrum of a 20 nm specimen. Reproduced with permission.[59] Copyright 2017, AIP Publishing.

The capability of perylene derivatives to grow in a quasi-epitaxial mode, once thermally evaporated under vacuum[60,61] on a variety of substrates, has been verified particularly for PTCDA on silver, a system whose structural, morphological, and electronic properties have been widely studied in the past.[67–69] When thin layers of PTCDA were deposited on Ag(110), the first ML showed a distorted arrangement with respect to the bulk structure, as confirmed by STM images.[70] Not a dissimilar situation occurs when thin films of PTCDA were epitaxially grown on Ag (111). Here a GIXRD experiment[22] permitted the indexing of the lattice parameters, again showing limited deviations with respect to those of the bulk α-polymorph.

In **Figure 3** the lattice phonon Raman spectrum of the powder of PTCDA is shown (bottom), and is assigned to the α-polymorph,[71] which is also the commercial product. The comparison with the data of phonons of the thin film (top part of the figure)[72] clearly shows a good matching between thin film and bulk phonons, confirming the evidence that no new structures appear in the film. Although by increasing the deposition temperature different morphologies were generated, they were all related to the same crystal structure, as confirmed by the low-frequency Raman spectra.[72]

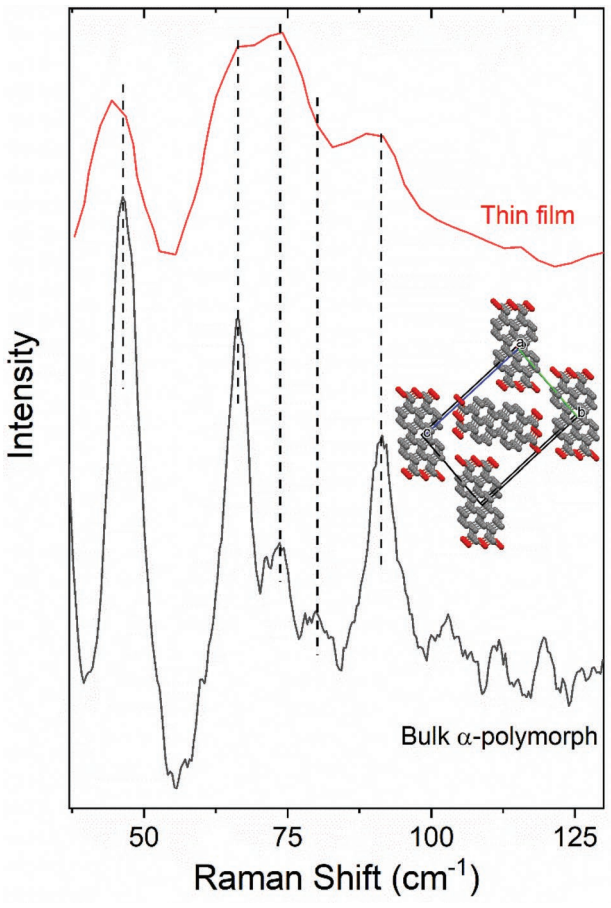

Figure 3. Bottom: Lattice phonon spectrum of the powder of the α-polymorph of PTCDA with its unit cell. Top: comparison with the spectrum of the thin film evaporated on H-Si(100) surface. Reproduced with permission.[72] Copyright 2000, Elsevier.

The fact that single crystals and thin films of PTCDA both share almost the same wavenumbers of the phonon peaks, as well similar lattice parameters, seems to be a strong indication that we are indeed dealing with distorted bulk structures for this class of materials.

2.2. Substrate-Selected Polymorphs

Contrary to the previous case, surface-selected polymorphs are stable and represent genuine new structures with no relationship to any known bulk form. The substrate may act as a template for an epitaxial growth or, alternatively, a new polymorph can result from the subtle play of the interactions between the molecular layers and the surface.

2.2.1. Pentacenequinone (PQ)

Two crystal structures have been reported for pentacene-quinone (PQ). A monoclinic one with two molecules per unit cell, $Z = 2$, found in the single crystals[73,74] and a triclinic surface-mediated phase with $Z = 1$, in films on native silicon oxide (SiO_x).[75] The latter, in some cases, can be found concomitant with the former one,[76] probably because the volume per molecule of the two structures differs of only 1.4%, with the single crystal phase being the denser one. Alike pentacene, the herring-bone molecular fashion of the bulk phase ends up with a standing up arrangement once the PQ units stick on the substrate, with a reduced number of molecules per unit cell. Comparison between the two structures shows a different plane texturing in the two structures, as detailed in ref. [75] whose consequence justifies the different molecular packing of the two polymorphs. Lastly, calculations of the corresponding cohesive energies, compared to the experimental enthalpy of sublimation, confirm that the SIP is a metastable phase.[75]

Within this framework, two distinctive lattice phonon Raman spectra are expected and, in fact, observed, as shown in **Figure 4**. In the upper part, the spectrum of a 30 nm film vapor deposited on SiO_x at a rate of 2 nm min^{-1} is shown and compared with the monoclinic bulk form (lower part). The SIP structure is obviously classified as a surface-selected polymorph.

The assignment of the Raman spectra is further facilitated by the pattern of Raman-active phonons expected on the basis of the number of molecules per unit cell: the three phonons of A-symmetry of the triclinic space group ($Z = 1$) split into three doublets of ($A_g + B_g$) symmetry in the monoclinic phase with $Z = 2$.[77] The Raman spectra are thus complete and the inter-molecular lattice phonons and the low-frequency intra-molecular modes do not mix, indicating that PQ behaves like a rigid molecule.

2.2.2. Perfluoropentacene (PFP)

Perfluoro-pentacene (PFP) is a typical n-type semiconductor belonging to the well-known class of pentacene derivatives. Also in this case, two polymorphs have been reported: the single

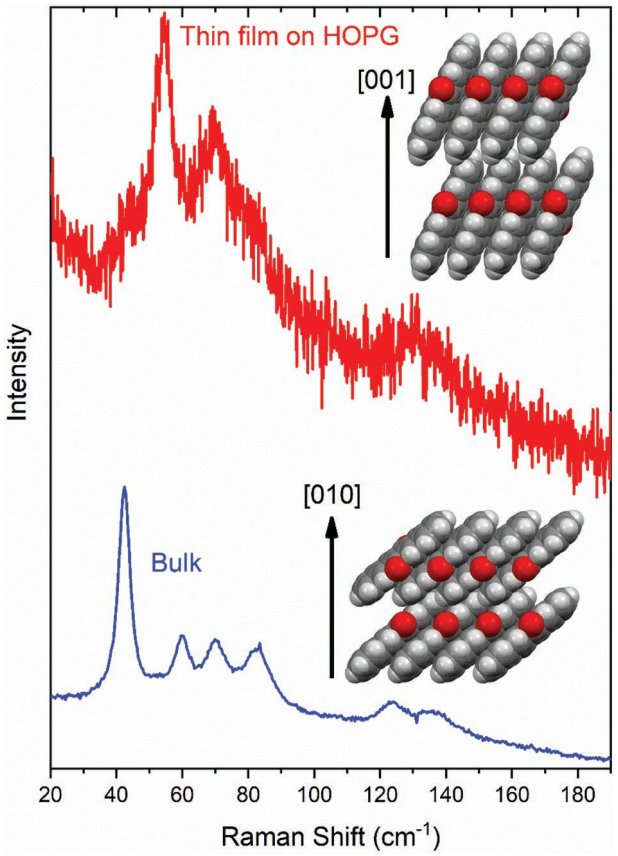

Figure 4. Lattice phonon Raman spectra of pentacene-quinone. Red: the substrate-selected phase, triclinic $Z = 1$; blue: the single crystal phase, monoclinic $Z = 2$. The molecular packing in the unit cell is also shown.

crystal structure[78] and a thin film structure.[18] Again, the bulk structure shows the common herring-bone arrangement, whereas in the thin film phase the molecules lie flat on the surface in a π-stacking fashion.[18] The latter structure is definitely a substrate-selected structure, being obtained via an epitaxial growth on graphene-coated quartz. The choice of the substrate is important in that, once films of PFP are deposited on native silicon oxide, the structure corresponds instead to that of the single crystal.[79] Due to the epitaxial nature of the SIP structure, no relationship can be found between the two polymorphic forms of PFP. In **Figure 5** the phonon spectra of both structures are shown.

As expected, and similarly to pentacene and PQ, also the spectra of PFP show two distinct profiles in the region of the lattice phonons (wavenumbers < 150 cm^{-1}), which allows for an easy and immediate polymorph identification.

2.2.3. Dibenzo-Tetrathiafulvalene (DB-TTF)

The last example of surface-selected polymorphs is that of dibenzo-tetrathiafulvalene (DB-TTF), an organic semiconductor for which four polymorphs have been found by lattice phonon confocal Raman microscopy.[80] For three of them, the XRD structure has been solved. **Figure 6**a shows the four distinctive phonon profiles.

Whereas the two monoclinic structures, α and β, had been solved by XRD,[80,82,83] the structure of the triclinic polymorph, δ, was found only later[84] and assigned on the basis of the correspondence of its lattice phonon spectrum previously recorded, a working example of phase recognition by Raman spectroscopy.[85] The structure of the fourth polymorph of DB-TTF, called γ, is still unknown, since no single crystals suitable for XRD analysis could be grown. In the attempt to solve this structure, thin films of DBTTF blended with polystyrene (PS) were deposited using the method of bar-assisted meniscus shearing (BAMS), obtaining either the α and γ phase or a mixture of them.[81] The crystal structure of the γ-phase was then characterized with specular XRD and GIXRD and, although a complete crystal structure could not be solved, a unit cell determination was nevertheless given. This phase showed up as a crystalline film with molecules standing upright on the substrate and a structure with two molecules per unit cell in a herring-bone fashion was hypothesized.[81] We therefore believe that the γ-phase is a genuine surface-selected structure, which grows only as a thin film, and does not show any correspondence with all the three other single crystal structures known.

As in ref. [81] we also had previously observed the attitude of an easy mixing between α and γ phase. There is also experimental evidence of the evolution of the γ to the α-phase by increasing coverage, pretty much as the TF phases of pentacene and tetracene when they turn to the bulk HT phase on increasing molecular deposition. This is shown in Figure 6b, where, starting from the pure γ phase, the phonon profiles, by increasing the amount of the material sublimed on the cold glass tip, soon evolve in a physical mixing of γ and α phases. At the same time large needle-shaped single crystal of the α polymorph start to grow on the top of the initial polycrystalline film. We then classify also the γ-phase of DBTTF as a surface-selected polymorph.

2.3. Substrate-Stabilized Polymorphs

Unlike the first two classes of polymorphs, where a real distinction can be recognized between bulk and substrate-mediated structures, in this category we observe structures, often metastable, that are stabilized by suitable surfaces, thus yielding what we call a substrate-stabilized polymorph. When prepared in their bulk form, they may also be found concomitant with other polymorphs, yielding a phase mixing. Some examples are given in the following sections and, for each of them, their peculiar behaviors will be illustrated.

2.3.1. C8O-BTBT-OC8 (2,7-dioctyloxy[1]benzothieno[3,2-b] benzothiophene)

The first example of a substrate-stabilized polymorph is that of the organic semiconductor C_8O-BTBT-OC_8. The compound, once crystallized from solution, shows two different morphologies, depending on the solvent and on the evaporation conditions.[86] From the XRD data only, it was unclear whether one of the two polymorphs was corresponding to the SIP previously reported.[87] The bulk phase shows a structure with a π–π slipped stacking

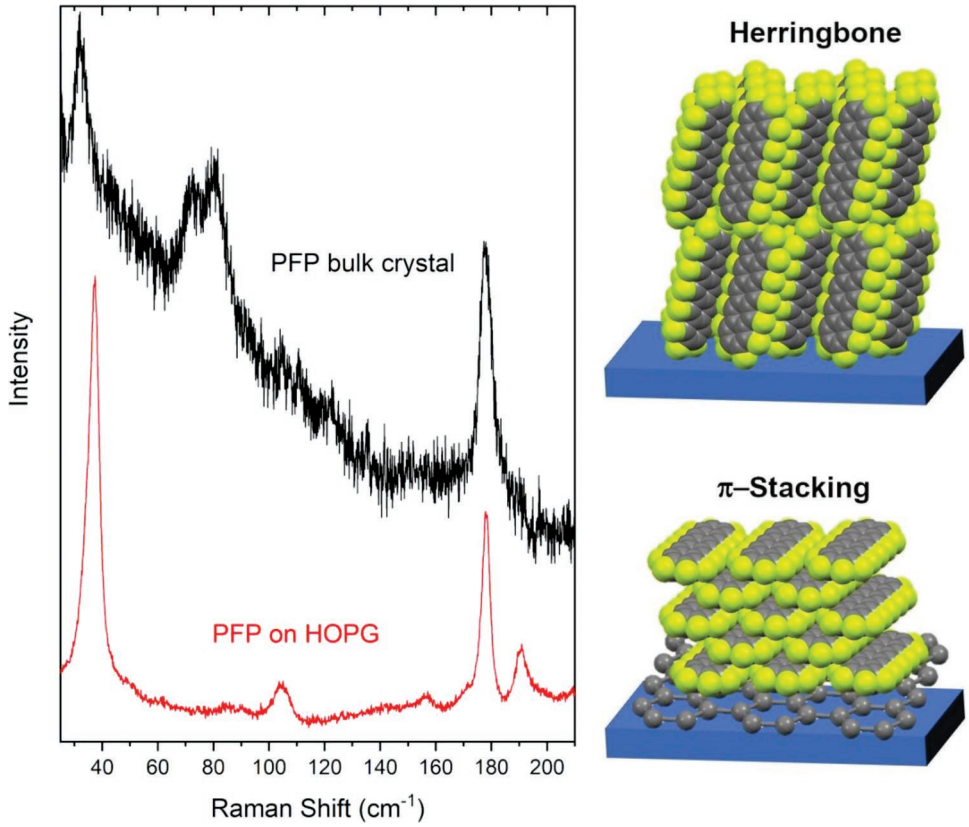

Figure 5. Distinctive lattice phonon spectra of the two known crystal structures of PFP: the bulk phase (above) and the surface-selected phase (below). The corresponding molecular packing are shown on the right. The nominal thickness of the PFP film is 30 nm.

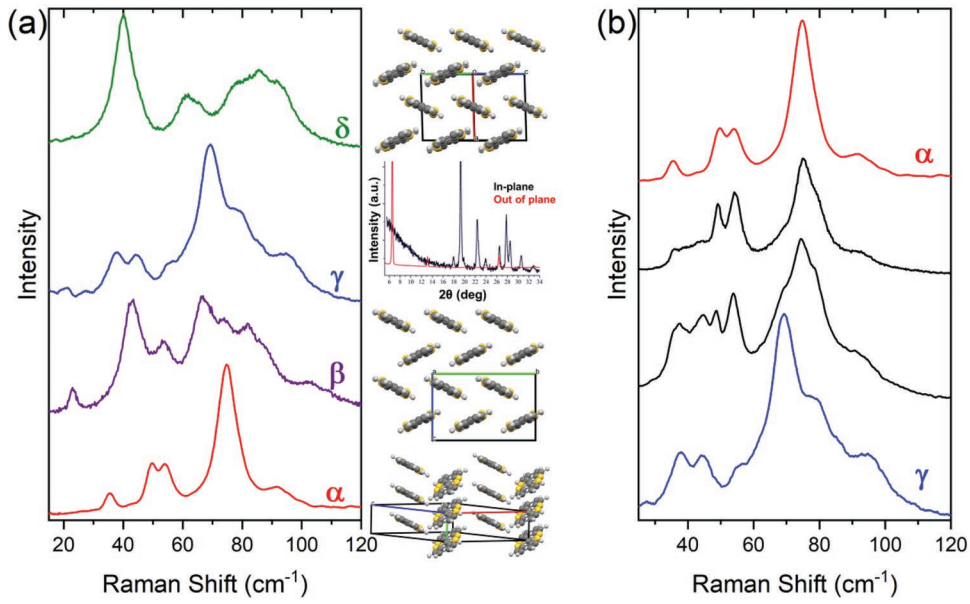

Figure 6. a) The four polymorphic modifications of DB-TTF, as recognized by their distinctive lattice phonon spectra. The corresponding unit cells, for the three bulk forms, are also shown; γ-phase is the surface-selected polymorph, whose complete structure has not been solved A possible unit cell by XRD reflectivity and GIXD was attempted,[81] see text. b) Evolution of lattice phonon Raman spectra of sublimed material on a cold glass tip from the γ to the α phase.[80] Intensities are shifted and normalized for a better comparison. Reproduced with permission.[80] Copyright 2008, The Royal Society of Chemistry.

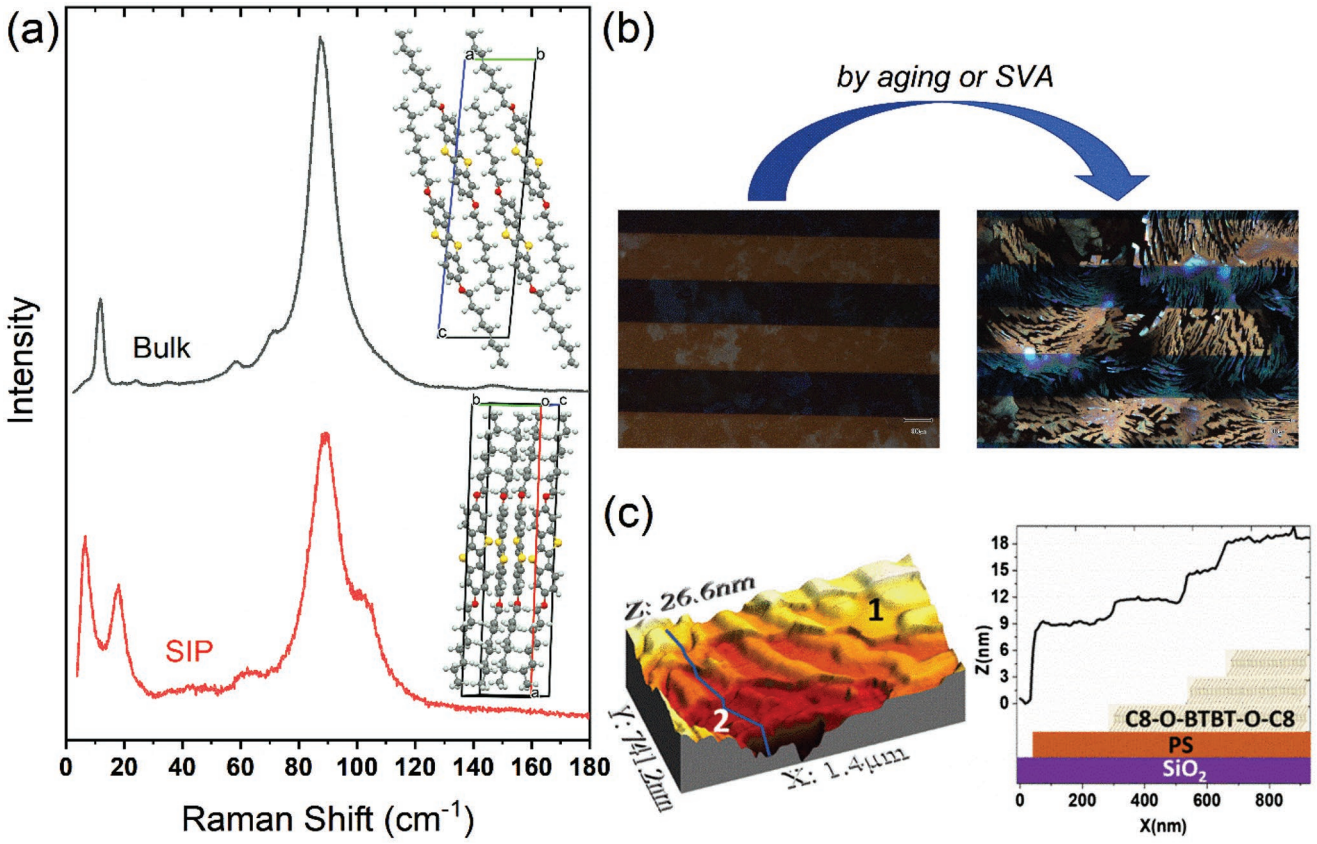

Figure 7. a) Lattice phonon spectra of the two polymorphs of C_8O-BTBT-OC_8 obtained from solution. The upper spectrum corresponds to the previously known bulk form, the lower one to the SIP. The corresponding structures are reported. b) thin film phase transformation SIP →Bulk accompanied by the morphological change. c) 3D representation of a topographic image of C_8O-BTBT-OC_8 polymer blend and its schematic profile taken at the line marked.[89] Reproduced with permission.[89] Copyright 2020, John Wiley and Sons.

motif, whereas the SIP presents the usual herring-bone molecular arrangement (inset of **Figure 7**a). It was therefore plausible to think that these marked differences in the molecular packing could lead to some distinctive features detectable by vibrational spectroscopy (IR and Raman). The details of this successful approach are reported elsewhere.[86] The point here is to show the efficiency of the lattice phonon spectra in discriminating the two polymorphic form. This is illustrated in Figure 7a, where two distinct spectral profiles produce an immediate phase recognition of the compound. In this very case the assistance of DFT calculations[88] was essential in assessing the spectral profile to the given structure: the lower spectrum corresponds to the SIP,[87] the upper one to the previously known bulk form.

Further investigations on the SIP showed its stability on solution processed films on silica surfaces at different experimental conditions.[87] By aging or post-treatment of the films by SVA (solvent vapor annealing) a morphological change was observed, as reported in Figure 7b, accompanied by the structural phase transition to that of the bulk, suggesting that the SIP phase is a metastable one.[86] In a recent work[89] thin films were prepared by solution shearing of C_8O-BTBT-OC_8 in polymer blend revealing a higher device performance with a field-effect mobility close to 1 $cm^2\ V^{-1}\ s^{-1}$, a threshold voltage close to 0 V, and an on/off current ratio above 10^7. In this work, in situ lattice phonon Raman microscopy was used to follow the stability of the SIP polymorph. Whereas films of the pure material showed the evolution from the SIP to the Bulk phase, in the blended samples no morphological and structural changes were observed. Besides, AFM (Figure 7c) demonstrated that the passivation of the silica surface by the polymer stabilized the SIP polymorph, leading to improved device performance and long-term stability. It is then concluded that the SIP of C_8O-BTBT-OC_8 is a typical case of surface-stabilized polymorph.

2.3.2. Paracetamol (N-(4-hydroxyphenyl)-acetamide)

Another compound that we like to include as exemplary of this category is a widely studied pharmaceutical ingredient, *N*-(4-hydroxyphenyl)-acetamide, better known as paracetamol and well recognized for his polymorphism. Paracetamol presents three polymorphs. Form I, the thermodynamically stable form, is monoclinic with $Z = 4$ and is the commercial compound used as a pharmaceutical drug on the market.[90] Form II and III are orthorhombic, with $Z = 8$.[91,92] They are both metastable, with the latter considered for long time an elusive form, solved only in 2009.

Following the procedure of previous compounds, in **Figure 8**a we report the phonon spectra of the three polymorphs, as revisited in a recent paper.[21]

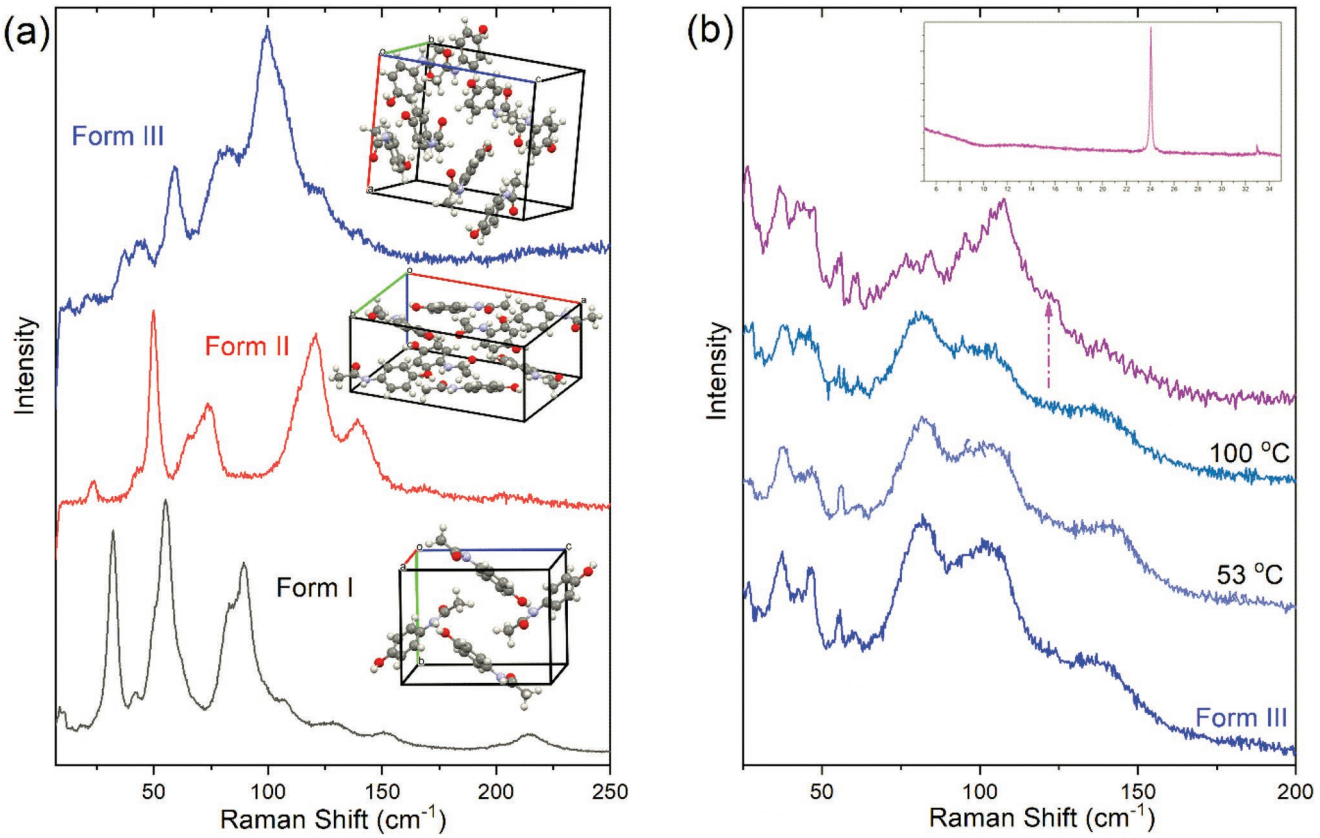

Figure 8. a) Lattice phonon spectra of the three polymorphic forms of paracetamol with their unit cell. b) Lattice phonon spectra of a paracetamol film spin coated on glass. The substrate-stabilized polymorph is the form III. The dashed arrow indicates the first appearance of form II by cooling after a thermal cycle up to 100 °C. In the inset on the top, the specular X-ray reflectivity of the same sample shows as a main feature the typical (004) peak of the form III. The silicon peak is the small feature at higher angles. Reproduced with permission.[21] Copyright 2018, American Chemical Society.

As to the surface mediated structures of paracetamol, a comprehensive account had been previously reported.[93] In this paper the stabilization of the metastable forms of paracetamol was studied with GIXRD on a spin coated film on a silica surface. Additional information was given on the film morphology, as well as on the organization of the molecular domains on the surface, textured according to the (001) plane. With this in mind, a subsequent Raman study[21] was carried on, with the aim to further confirm the effect of the substrate in selecting and stabilizing the polymorph III, otherwise metastable once in the form of powder or single crystal.

Spin-coated films of paracetamol were deposited on glass, gold and polystyrene substrates, invariably yielding the metastable form III which showed an unprecedented stability over a time span of several months. Form III is then the substrate-stabilized polymorph of paracetamol. This is represented with typical spectra of spin coated films on glass in Figure 8b. Only after heating up to 100 °C and subsequent slow cooling, form II started to appear (dashed arrow in the Figure 8b). In inset of the figure, the specular reflectivity of the film confirmed the typical (004) peak of form III.[21] It is once more important to remark that by exploiting the complementary Raman and XRD techniques it is possible to assign each phonon spectrum to its corresponding crystal structure making easier polymorph recognition.[29]

2.3.3. Thioindigo (2-(3-Oxo-1-benzothiophen-2(3H)-ylidene)-1-benzothiophen-3(2H)-one)

The polymorphism of a number of natural dyes, functional to the manufacture of OFETs, has been studied in the last years and very recently summarized.[27,94] Most of these structures show peculiar properties once deposited on suitable technological substrates,[95–97] resulting in the stabilization of the metastable forms on the surface. The example shortly reported here is thioindigo (2-(3-Oxo-1-benzothiophen-2(3*H*)-ylidene)-1-benzothiophen-3(2*H*)-one), that displays two polymorphs, α and β, both monoclinic with two molecules per unit cell.[98,99] The phonon spectra of the two bulk forms are shown in **Figure 9**a. It is interesting to notice that the α and β phases appear concomitant under a number of growth conditions, probably due to their structural similarity. In any case, polymorph β is always predominant in thermodynamic growth conditions such as vapor method (sublimation or physical vapor transport—PVT), whereas the α phase is the one preferentially growing in non-thermodynamic conditions as drop-casting or spin-coating on substrates, then falling into the class of surface-stabilized polymorphs.[20] A way to stabilize and to obtain the pure α-polymorph is to prepare thin film in a controlled manner by solution shearing technique at selected speed and substrate temperature. The substrate-stabilized α-polymorph

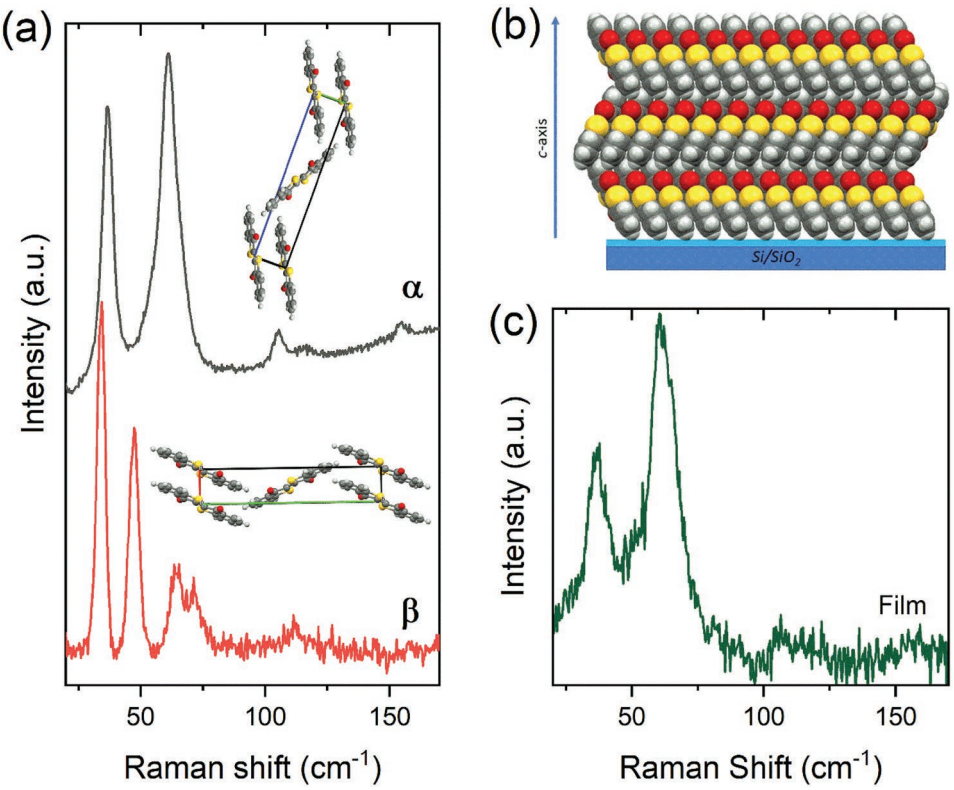

Figure 9. a) Unpolarized phonon spectra of α and β polymorph of thioindigo with their unit cells. b) Molecular packing of the film stacked perpendicular to the *c*-axis. c) Polarized spectra of the surface stabilized α-phase of thioindigo films obtained with the BAMS method.

presents highly homogeneous and well-ordered films once they are prepared by means of the BAMS method.[100] Its spectroscopic characterization, assisted by DTF computations, is fully accounted elsewhere,[20] The molecular packing of the obtained pure α-polymorph film and its phonon spectrum are shown in Figure 9b and c, respectively.

2.4. The Case of α-Sexithiophene (T6)

We mention here the case of another classical semiconducting material, widely used for its applications in organic electronics: α-sexithiophene (T6).[101,102] The two polymorphs of T6 are known as LT[103] and HT,[104] according to their temperature of growth. At intermediate temperatures they easily undergo phase mixing, revealed in the confocal Raman configuration, also by penetrating the bulk from the surface.[105] The two T6 phases are both monoclinic, and differ in the number of molecules per the unit cell, $Z = 2$ and $Z = 4$ for HT and LT, respectively.

Though scarcely mentioned, T6 does show a thin film phase, formed by molecules standing normal to the substrate with a unit cell different from that of the bulk.[106] The same study indicates that T6 grows as disordered crystalline layers since the beginning of the evaporation. This disordered layered phase in thin films was confirmed in a subsequent work[107] and the evaporation rate of vacuum deposited T6 revealed strong analogies with pentacene and tetracene. In fact, it was reported that at low rates the 3D thermodynamically stable LT phase was obtained, whereas the thin film phase was favored at high rates. The latter phase, kinetically induced, displayed typical features of 2D crystals, which are laterally ordered but without interlayer correlations of the molecular positions.[107]

We then performed the confocal Raman analysis of films deposited on Si/SiO_x. **Figure 10**a shows that up to 8 ML (nominal thickness 20 nm) no signal is detected in the lattice phonon region, whereas the internal modes, Figure 10b, are already well detectable in a sample of 2 ML (nominally 5 nm).[105] Only at 16 ML a phonon structure appears and corresponds to that expected for the LT polymorph. This is in agreement with previous work.[106,107] The lack of the Raman signal of the lattice modes is then easily explained by the disordered structure of the first few MLs, which do not possess the periodicity to allow the phase matching necessary to obtain the propagation of phonons, as typical for disordered systems.[108] By increasing the number of MLs the molecules gradually tilt, up to reach the LT structure of the bulk crystal when the full phonon spectrum appears. This is represented in Figure 10c, where a sketch of the molecular deposition on the substrate is symbolically visualized. The intramolecular modes are instead always detectable, down to 2 ML, testifying the molecular identity of the deposited material. This point will be further recalled in a following section.

3. Three Experiments on the Interaction between the Molecular Layers and the Substrate

The interaction between the substrate and the layered structure of a film, as well as at the contact interface, falls in the general

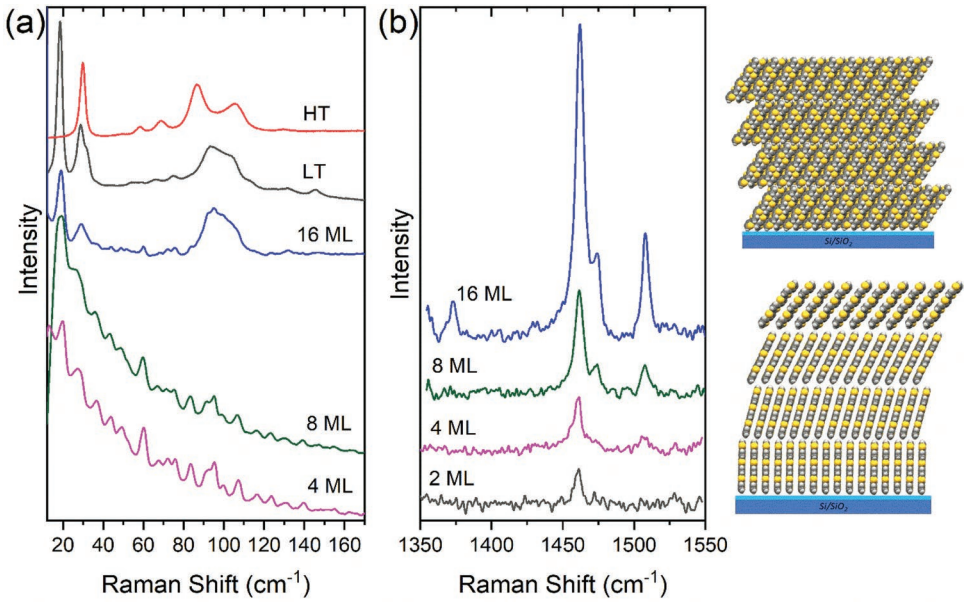

Figure 10. a) Evolution from the disordered film structure to the bulk LT polymorph as seen from the optical phonon spectrum of T6. b) A selected intramolecular spectral region from 2 to 16 ML. A visual representation of the disordered structure ending up to the LT phase is given at the right.

framework of interfacial phenomena at the boundary between two contiguous media. Similarly to other physical phenomena, the nature of the substrate and that of the deposited compound are, separately, important in producing distinct contributions to the properties of the system. However, when the system is considered as a whole, the nature of the interface becomes the origin of new properties, not otherwise present in the two separate systems, the molecules and the surface. Just to mention an example involving Raman spectroscopy, SERS (surface-enhanced-Raman-scattering) is a pertinent one. In fact, in this very case, the molecules and the surface, separately, play a distinct role, but the molecules on the surface open the way to a variety of new striking phenomena.[109–111] In a similar way, an insulator, once interfaced to a metal or to a semiconductor, acquires the properties of a new system with a partial or complete loss of its original nature.[112–114] In other words, we must be aware that few molecular layers on a surface constitute a novel system, where the subtle play of weak interactions at the interface leads to new molecular architectures with properties often unexpected in the bulk, but functional to improve the transport properties of the active layer.

Without getting into a detailed description of phenomena otherwise treated in a vast literature, we just mention three experiments involving charge transport at the interface, as well as how far the effect of the surface goes and when a transition from an SIP to the bulk phase takes place.

3.1. Carrier Mobility

The understanding of the nature of charge carriers at the semiconductor/dielectric interface is a key factor in the structure-property relationship finalized to obtain high performance organic field-effect transistors (OFET).[115] Hole mobility in OFET was studied as a function of coverage in T6,[13] dihexylquaterthienyl,[116] and pentacene.[14]

Figure 11a shows that the charge carrier mobility of T6 rapidly increases with coverage and saturates at about 2 ML (5 nm of nominal thickness),[13] implying that it is strictly confined at the interface. This result was later confirmed for pentacene,[14] as shown in the lower part of Figure 11b. Besides, the saturation thickness is clearly rate dependent. Also in this case, it reaches a maximum at 2 ML, then it decreases, making clear the point that charge carriers flow mostly in the very first molecular layers next to the dielectric.[14]

It is then confirmed the complex role of the nanoscale engineering at the interface, whose importance increases as device dimensions shrink to the scale of very few MLs.[117] Consequently, the structure of a SIP becomes one of the most critical factors in determining the optimal charge transport properties of the electronic device.

3.2. How Far the Effect of the Surface Goes

This experiment wants to show how far the effect of the surface is perceived by the molecular layers and dates back some 15 years ago.[105] It is based on the Raman signal of the strongest internal mode of T6 at about 1460 cm^{-1}. The organic semiconductor was vacuum evaporated on a series of microfabricated test patterns as prototypes of T6-based OFETs and the entire surface was measured point by point by means of confocal Raman microscopy, up to obtain a series of maps of the outcoming Raman signal. The nominal molecular coverage of the samples was 10, 25, and 62.5 nm, corresponding to 4, 10, and 25 ML, respectively. We found that the intensity of the Raman signal of T6 was systematically larger on the gold electrodes than inside the channels. We believe that the most likely explanation relies on the higher sticking coefficient of T6 molecules on Au electrodes, with respect to the HMDS-coated channel, which causes a larger nucleation density (viz., number

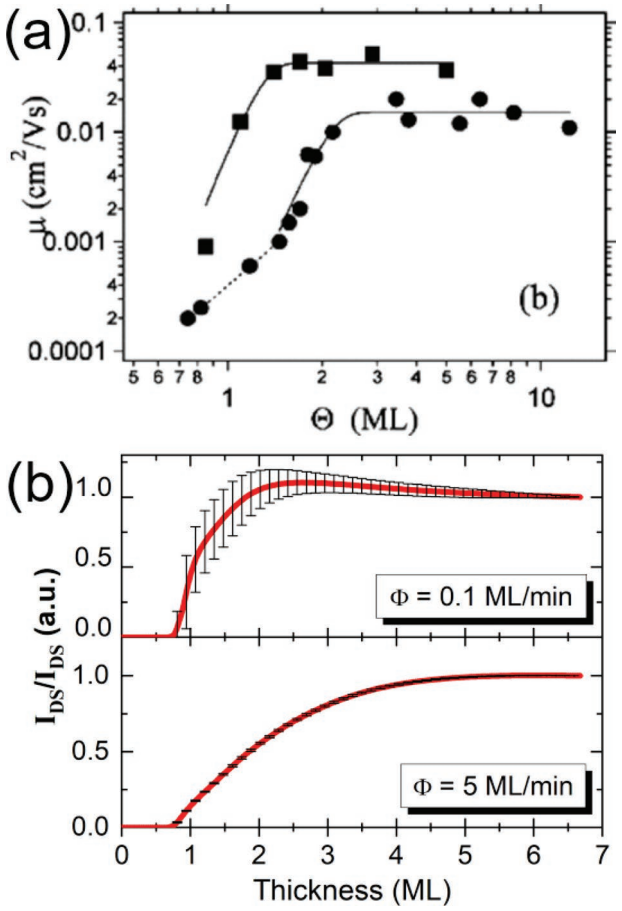

Figure 11. a) Hole mobility versus coverage in a p-type T6 FET operating device. Reproduced with permission.[13] Copyright 2004, American Physical Society. b) Drain-source current versus ML during the growth of pentacene thin films at deposition rates 0.1 and 5 ML min^{-1}. Reproduced with permission.[14] Copyright 2010, American Physical Society.

of domains or grains per unit area) on the Au electrodes with respect to the channel for the growth conditions used, as evident from Figure 7b of ref. [105]. It is therefore possible to reproduce, with a false color palette, the pattern of the devices with a molecular Raman map. We can readily see that **Figure 12** shows an overall good matching between optical images and Raman maps for the sample of 10 nm, and this still reasonably holds for the 25 nm thickness of T6. Once looking at the 60 nm coverage, a clear mismatch is observable between the optical and the Raman map. It was concluded that on increasing thickness of the deposited material the template effect given by the patterned electrodes is gradually lost and, by further coverage, the T6 growth proceeds in a homo-epitaxial mode.[118]

This behavior was consistently confirmed with a large number of samples, and, although limited to T6, yields an experimental estimate of the interactions at the boundary molecule/surface, roughly indicating that only up to about 25 nm from the substrate the molecular memory is maintained.

Lastly, it is worth to notice that these Raman maps are a skillful tool to assess the uniformity of the multilayer depositions in thin films and OFET, constituting a sound method to control both crystal structure and molecular growth on surfaces.

3.3. When Is the Bulk: The Transition from a Thin Film to the Bulk Crystal

The problem of the transition from a thin film to a bulk structure has got, contrary to the previous experiments, quite a reasonable feedback in the literature. The paper of Jones[87] can still be the starting point of this issue. However, we shall preferentially show here the experiments on T6 and pentacene, two classical organic semiconductors already treated in the previous sections.

The growth of T6 on SiO_x has been investigated in the past,[106] and GIXRD spectra were detected on increasing deposition of T6 layers. The experiments showed that the molecules, initially oriented perpendicular to the substrate, gradually bend by increasing coverage, up to reaching the LT single crystal structure.[106] The onset of the appearance of the bulk structure was, with a deposition rate of ≈0.04 Å s^{-1}, at about 6 ML, corresponding to a nominal thickness of 15 nm, a value not too far from that observed in the Raman experiment of Figure 10a, although the disordered nature of the film makes difficult a straight comparison between the two techniques.

More detailed is the case of pentacene. In **Figure 13** a similar experiment was performed with specular XRD patterns as a function of coverage at three different deposition rates.

The structures of the different films grown at the deposition rates as indicated in the figure show that the films were polycrystalline, with the *ab* layers parallel to the substrate. The thinner films (up to 30 MLs) consist only of the TF form. On increasing thickness the TF and HT bulk phases start to coexist,[42,52,53] an observation that subsequently was also found for the TF and bulk phases of tetracene.[59] An important remark is that the onset of the transition from TF to HT polymorph is strongly rate dependent: the lower is the deposition rate, the lower is the onset of the HT phase, consistently with the 3D regime associated to the lower rates.

To compare these data with the Raman measurements, we report in **Figure 14** the intensity of the C—H bending intramolecular mode of pentacene, detected for selected film thicknesses.

The figure shows that the transition from thin film to bulk occurs between 30 and 50 ML, at a deposition rate Φ = 0.033 Å s^{-1}, exactly matching the value found from the GIXRD data at the same rate. It is notable to outline that in this case XRD and Raman data completely agree as to the coverage which determine the transition. The value from 30 to 50 ML for both cases (compare Figures 13 and 14), is a further impressing evidence of the excellent agreement between XRD and THz Raman techniques for structure recognition.

As a final comment, we remark that throughout the paper, we have widely used the expression "thin film" and "thin film structure," following the mainstream of a consolidated literature in the field. However, from a physical point of view, this expression, if not vague, is certainly not quantitative. We then need to find a criterion to give a more focused answer to the question on what do we really mean as a thin film: how thin is "thin"?

Going back to the experiments described here and in the previous sections, we can roughly estimate that a thin film structure, or a SIP, could be expected within 50 nm from the surface or even less. From the point of view of the charge transport, instead, the active semiconducting layer is much closer to the substrate,[13–16] in any case well below 10 nm, namely, an

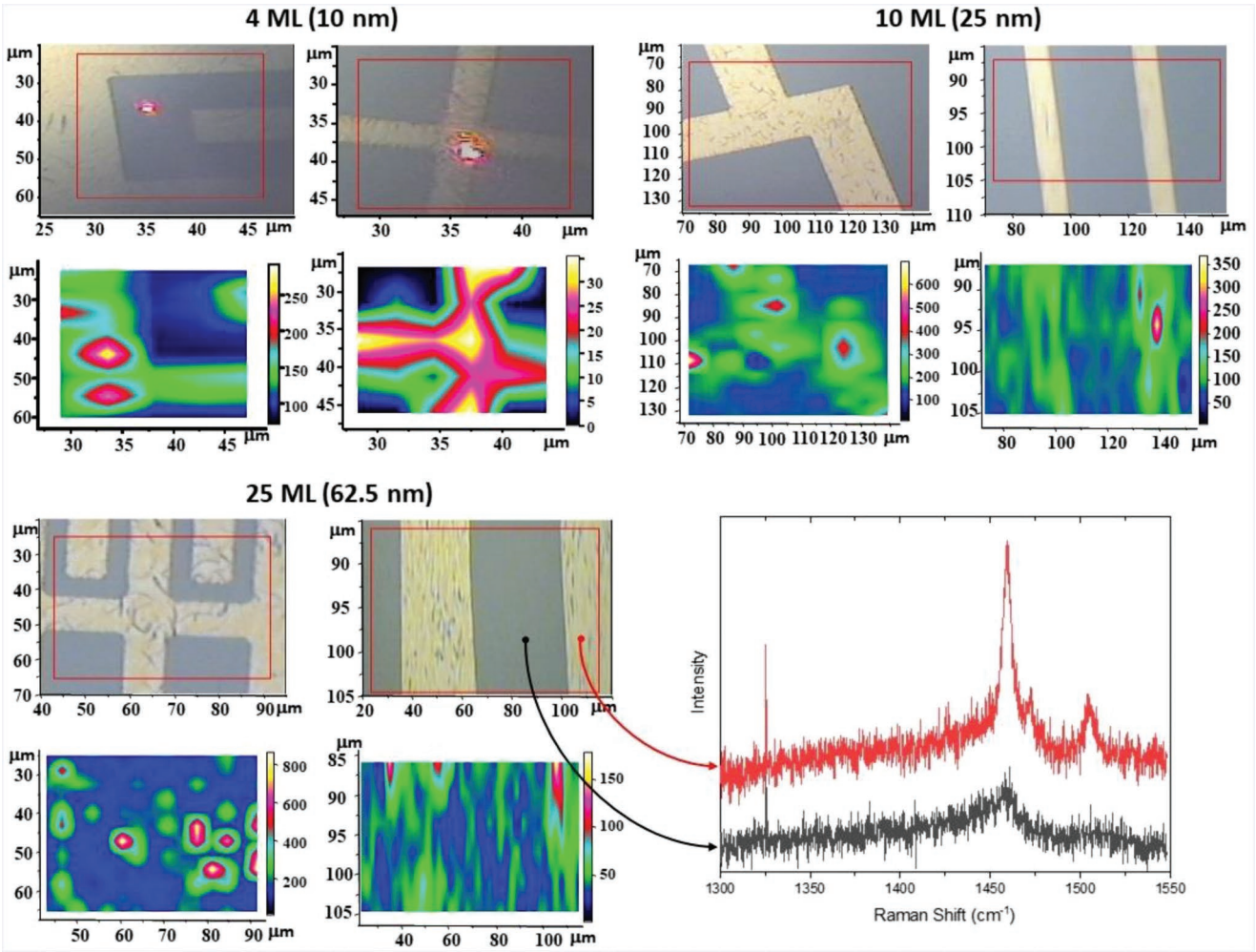

Figure 12. Comparison between microscopic images and confocal Raman mapping of test patterned devices based on T6 films grown with a different amount of molecular deposition: 4, 10, and 25 ML respectively. The last panel shows a typical Raman signal of T6 in OFETs, on the gold electrode (red arrow) and inside the channel (black arrow).

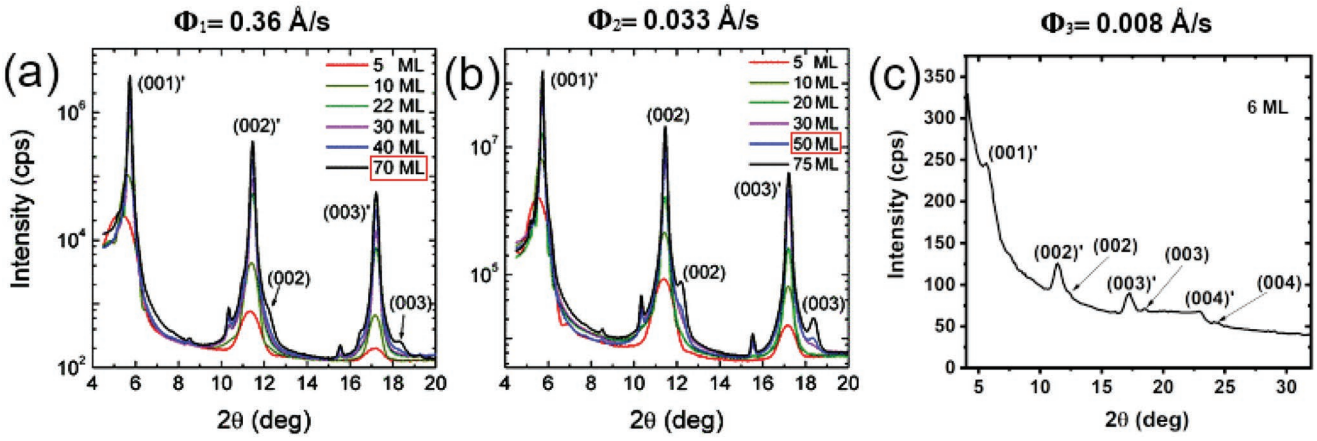

Figure 13. a,b) Specular XRD patterns of pentacene films grown on SiO_2 at rates $\Phi_1 = 0.36$ Å s^{-1} and $\Phi_2 = 0.033$ Å s^{-1}, for a series of samples in the range 5–75 ML. Reproduced with permission.[85] Copyright 2012, American Physical Society c): Specular XRD pattern of a 6 ML film with interlayer distance of 15.45 Å (TF polymorph) grown at $\Phi_3 = 0.008$ Å s^{-1}.[48] The small black arrows mark the onset of the HT phase. Reproduced with permission.[48] Copyright 2016, MDPI.

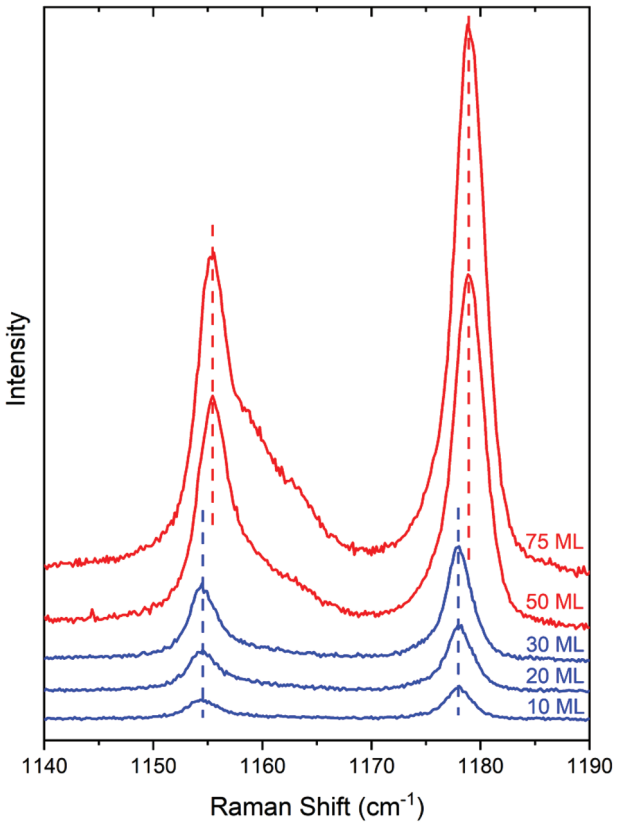

Figure 14. Raman spectra in the region of C—H bending of pentacene films grown on SiO_2 at rate $\Phi = 0.033$ Å s^{-1} ($\lambda_{exc} = 752.5$ nm). Thickness is indicated in MLs. The blue to red profiles mark the onset of the transition from the TF to the HT phase.

ultrathin film. Therefore, carriers are specifically active at the interface, whereas surface-mediated structures are built as long as the memory of the substrate is felt, that is, within 50 nm or less. These are the upper limits, in our opinion, to define a layered structure as a "thin film" for carrier mobility and SIP structures, respectively. By no way we want to claim this is a general statement for molecular materials, since we are well aware that the experiments described here refer to the only cases, though widely studied and highly representative, of pentacene[48,85] and T6.[105,106] Besides, this statement may not be assumed irrespective of the kind of substrate, the preparation conditions and some important growth parameters, such as the deposition rate. Our main goal is to stimulate further experiments on other organic semiconductors to improve the knowledge of their properties at the interface with the substrate.

Finally, pentacene still remains a model system for the description of phenomena dealing with increasing coverage at the interface: it starts with a structure of a single ML,[39] then forms ultrathin films for hole and electron transfer, thin films for its SIP structures and eventually bulk single crystals.

4. Toward 2D Phonons in Molecular Crystals

Structural properties (surface-mediated structures) and collective excitations, such as optical phonons in systems of reduced dimensionality, belong to the fascinating world where the properties of materials may end up in new physical phenomena. This has been discussed in a recent perspective[119] that deeply investigates the properties of new synthesized 2D materials and hetero-structures, describing their behavior in optimizing new and unexpected physical properties and applications. These compounds are formed by 2D atomic layers, therefore are mostly related to inorganic materials. A similar study for 2D molecular crystals is still lacking and the only molecular systems insofar treated, to our knowledge, are limited to 0D molecules such as fullerene[120] or to the unique 2D case of graphene.[121]

We believe that ultrathin films down to 1 ML or to sub-ML may represent what is closer to a 2D molecular structured material. Therefore, SIP (structures) and phonons (dynamics) both represent the ideal benchmark for a discussion on 2D molecular crystals.

There is now solid evidence on the morphological growth of organic material in different dimensional regimes, with the transition from 3D to 2D essentially related to temperature and deposition rate (Φ) during the vapor growth of the film on the substrate. This has been shown for pentacene,[26,47] tetracene,[59] and T6.[106,107] The general trend is that there is a definite change in the dimensionality from 3D to 2D on increasing Φ,[14,47] in agreement with previous data on nucleation and growth appeared in the literature.[13,51,116] Phonon dynamics is also affected, and manifests in a drastic change of the THz Raman profiles, whose information lie in the theoretical curves of phonon dispersions $\omega(\mathbf{k})$, with ω and $\mathbf{k}$ being the phonon frequency and its wavevector, respectively.[47] We believe this is an important example of the so called dimensional disorder in a molecular crystal.[122]

An introductory discussion on 3D and 2D lattice phonons in a film structure of pentacene on SiO_x has very recently appeared and a full account has been given.[26] Here we just mention that the 2D regime in films of pentacene has been discussed in the general framework of a particular case of static disorder, called low-dimensional disorder,[122] specifically indicating how the dimensionality is strictly related to the dispersion of the lattice modes and to the interactions within and between layers. The loss of inter-layer order determines a loss of correlation among layers perpendicular to the substrate constraining the periodicity to very few ML, the ideal situation for a quasi-2D system.

When the disorder affects the dimensionality of the system, there is a further concept to be pointed out related to the film structure: the effective correlation thickness. Since the lack of order implies the lack of periodicity as well, an effective thickness of the film must then be considered, and needs to be connected to the length of correlation among layers, independently of the actual coverage on the substrate. When this correlation is lost, or even partially lost, as in the films grown at the high rates, the effective thickness is lowered down to only those few layers where the periodicity still holds.[26] This is a crucial point for the spreading of collective excitations like phonons or excitons, which propagate periodically and whose phase matching between layers is lost once a mismatch is produced by the vertical interlayer disorder.[47] The related example previously given for T6 can now be better explained. It was observed that the molecules, initially oriented perpendicular to the substrate, gradually bend by increasing coverage, up to reaching the LT single crystal structure (see Figure 11).[106] Strictly speaking,

the periodic vertical correlation among layers is lost and the "effective thickness" cannot correspond to the nominal thickness of the film. This is the reason why, XRD still shows a signal of crystallinity, although in a partially disordered structure. On the contrary, disordered, or amorphous, solids lacking long-range order cannot exhibit a definite lattice phonon pattern.[108] The Raman scattering, probing local order, gives information different from those of X-ray standard diffraction which probes the average, long-range order. The related X-ray diffuse scattering techniques should be used for this purpose.[123]

5. Conclusion

Surface-mediated structures of molecular crystals is an important new field in materials science, which has been investigated with advanced GIXRD techniques.[23] Molecular deposition on selected substrates is capable to induce specific polymorphs, either as bulk structures (surface-stabilized polymorphs) or as new forms (surface mediated structures). This survey aims to tackle the problem from the different point of view of low-frequency (5–150 cm^{-1}) lattice phonons, or THz Raman scattering (0.2–5 THz), to show that in some peculiar respects structure and dynamics are two complementary aspects in the physics of a material. Together with morphological analyses and computational assistance, it is evident that the approach to polymorphism must necessarily be multidisciplinary.

We have started classifying the structures at the interfaces in three main categories, surface-induced, surface-selected, and surface-stabilized polymorphs. This was done with the purpose to rationalize, and in a way to simplify, a subject which surely is facing a rapid expansion, playing a role in some important technological applications such as organic electronics and pharmaceutics.

We have then treated some experiments of recent years, with the purpose to agree on some general definitions such as "thin film" and "effective film thickness," ending up with a description that is not necessarily the same when dealing with different matters, such as carrier transport, crystal structures, or phonon dynamics. We also have used ultrathin films, down to a single ML, as a route to rationalize 2D structures and dynamics of organic materials in terms of the static disorder commonly called low-dimensional disorder.[26,122]

This paper, though mostly focused on optical lattice phonon dynamics, wants nevertheless to be a starting point to promote further experiments and theoretical descriptions on the exciting field of structures on surfaces. The problem of the phenomena at the interfaces, a hot topic since many decades, is certainly meant to remain one of the most crucial issues in the future of materials science.

Acknowledgements

The authors warmly thank Ingo Salzmann (Concordia University, Montreal) for the films of PQ and PFP and for discussions. The authors also thank their colleagues Elisabetta Venuti, Raffaele Guido Della Valle (Solid State Group of the Toso Montanari Dept, University of Bologna) who shared a large part of the research described in the paper.

Open access funding provided by Universita degli Studi di Bologna within the CRUI-CARE Agreement.

Conflict of Interest

The authors declare no conflict of interest.

Keywords

2D phonons, lattice phonons, low-dimensional disorder, polymorphism, structures at interfaces, substrate-induced polymorphs, substrate-mediated structures

Received: April 13, 2022
Revised: June 1, 2022
Published online: September 2, 2022

[1] J. Bernstein, *Polymorphism in Molecular Crystals*, Oxford University Press, Oxford **2007**.
[2] *Polymorphism in Pharmaceutical Solids*, (Ed: H. G. Brittain), CRC Press, Boca Raton, FL **2018**.
[3] D. Gentili, M. Gazzano, M. Melucci, D. Jones, M. Cavallini, *Chem. Soc. Rev.* **2019**, *48*, 2502.
[4] H. Chung, Y. Diao, *J. Mater. Chem. C* **2016**, *4*, 3915.
[5] P. Samorì, F. Cacialli, *Functional Supramolecular Architectures: For Organic Electronics and Nanotechnology*, Wiley-VCH, Hoboken, NJ **2014**.
[6] G. R. Desiraju, *Crystal Engineering: The Design of Organic Solids*, Elsevier, Amsterdam **1989**.
[7] A. K. Nangia, G. R. Desiraju, *Angew. Chem., Int. Ed.* **2019**, *58*, 4100.
[8] C. R. Taylor, M. T. Mulvee, D. S. Perenyi, M. R. Probert, G. M. Day, J. W. Steed, *J. Am. Chem. Soc.* **2020**, *142*, 16668.
[9] J. Bernstein, *Cryst. Growth Des.* **2011**, *11*, 632.
[10] A. O. F. Jones, B. Chattopadhyay, Y. H. Geerts, R. Resel, *Adv. Funct. Mater.* **2016**, *26*, 2233.
[11] 383th WE-Heraeus-Seminar Physics of Highly Ordered Organic Interfaces and Layers, Physikzentrum Bad Honnef, Germany, http://www.pbh.de (accessed: January 2007).
[12] 8th Workshop on Substrate-Mediated Polymorphism in Organic Thin Films, Berlin, Germany, http://smp2016.physik.hu-berlin.de/ (accessed: October 2016).
[13] F. Dinelli, M. Murgia, P. Levy, M. Cavallini, F. Biscarini, D. M. de Leeuw, *Phys. Rev. Lett.* **2004**, *92*, 116802.
[14] A. Shehu, S. D. Quiroga, P. D'Angelo, C. Albonetti, F. Borgatti, M. Murgia, A. Scorzoni, P. Stoliar, F. Biscarini, *Phys. Rev. Lett.* **2010**, *104*, 246602.
[15] R. Lassnig, B. Striedinger, M. Hollerer, A. Fian, B. Stadlober, A. Winkler, *J. Appl. Phys.* **2014**, *116*, 114508.
[16] Y. Fan, J. Liu, W. Hu, Y. Liu, L. Jiang, *J. Mater. Chem. C* **2020**, *8*, 13154.
[17] F. Calcinelli, A. Jeindl, L. Hörmann, S. Ghan, H. Oberhofer, O. T. Hofmann, *J. Phys. Chem. C* **2022**, *126*, 2868.
[18] I. Salzmann, A. Moser, M. Oehzelt, T. Breuer, X. Feng, Z.-Y. Juang, D. Nabok, R. G. Della Valle, S. Duhm, G. Heimel, A. Brillante, E. Venuti, I. Bilotti, C. Christodoulou, J. Frisch, P. Puschnig, C. Draxl, G. Witte, K. Müllen, N. Koch, *ACS Nano* **2012**, *6*, 10874.
[19] Y. Hao, G. Velpula, M. Kaltenegger, W. R. Bodlos, F. Vibert, K. S. Mali, S. De Feyter, R. Resel, Y. H. Geerts, S. Van Aert, D. Beljonne, R. Lazzaroni, *Chem. Mater.* **2022**, *34*, 2238.
[20] A. Rivalta, A. Giunchi, L. Pandolfi, T. Salzillo, S. d'Agostino, O. Werzer, B. Schrode, N. Demitri, M. Mas-Torrent, A. Brillante, R. G. Dell, V. E. Venuti, *Dyes Pigm.* **2020**, *172*, 107847.
[21] A. Rivalta, T. Salzillo, E. Venuti, R. G. Della Valle, B. Sokolovič, O. Werzer, A. Brillante, *ACS Omega* **2018**, *3*, 9564.
[22] J. Simbrunner, B. Schrode, S. Hofer, J. Domke, T. Fritz, R. Forker, R. Resel, *J. Phys. Chem. C* **2021**, *125*, 618.

[23] J. Simbrunner, B. Schrode, J. Domke, T. Fritz, I. Salzmann, R. Resel, *Acta Cryst. A* **2020**, *76*, 345.
[24] S. C. B. Mannsfeld, T. Fritz, *Mod. Phys. Lett. B* **2006**, *20*, 585.
[25] A. Winkler, *Surf. Sci.* **2016**, *652*, 367.
[26] T. Salzillo, A. Brillante, A. Girlando, *J. Mater. Chem. C* **2021**, *9*, 10677.
[27] T. Salzillo, A. Giunchi, L. Pandolfi, A. Brillante, E. Venuti, *Isr. J. Chem.* **2021**, *61*, 650.
[28] A. Brillante, I. Bilotti, R. G. Della Valle, E. Venuti, M. Masino, A. Girlando, *Adv. Mater.* **2005**, *17*, 2549.
[29] A. Brillante, I. Bilotti, R. G. Della Valle, E. Venuti, A. Girlando, *CrystEngComm* **2008**, *10*, 937.
[30] R. Ruiz, D. Choudhary, B. Nickel, T. Toccoli, K.-C. Chang, A. C. Mayer, P. Clancy, J. M. Blakely, R. L. Headrick, S. Iannotta, G. G. Malliaras, *Chem. Mater.* **2004**, *16*, 4497.
[31] R. B. Campbell, J. M. Robertson, J. Trotter, *Acta Cryst.* **1962**, *15*, 289.
[32] D. Holmes, S. Kumaraswamy, A. J. Matzger, K. P. C. Vollhardt, *Chem. – Eur. J.* **1999**, *5*, 3399.
[33] C. C. Mattheus, A. B. Dros, J. Baas, A. Meetsma, J. L. de Boer, T. T. M. Palstra, *Acta Cryst. C* **2001**, *57*, 939.
[34] T. Siegrist, C. Besnard, S. Haas, M. Schiltz, P. Pattison, D. Chernyshov, B. Batlogg, C. Kloc, *Adv. Mater.* **2007**, *19*, 2079.
[35] S. Schiefer, M. Huth, A. Dobrinevski, B. Nickel, *J. Am. Chem. Soc.* **2007**, *129*, 10316.
[36] H. Yoshida, K. Inaba, N. Sato, *Appl. Phys. Lett.* **2007**, *90*, 181930.
[37] D. Nabok, P. Puschnig, C. Ambrosch-Draxl, O. Werzer, R. Resel, D.-M. Smilgies, *Phys. Rev. B* **2007**, *76*, 235322.
[38] J. S. Wu, J. C. H. Spence, *J. Appl. Cryst.* **2004**, *37*, 78.
[39] S. E. Fritz, S. M. Martin, C. D. Frisbie, M. D. Ward, M. F. Toney, *J. Am. Chem. Soc.* **2004**, *126*, 4084.
[40] S. C. B. Mannsfeld, A. Virkar, C. Reese, M. F. Toney, Z. Bao, *Adv. Mater.* **2009**, *21*, 2294.
[41] A. Brillante, R. Della Valle, L. Farina, A. Girlando, M. Masino, E. Venuti, *Chem. Phys. Lett.* **2002**, *357*, 32.
[42] C. D. Dimitrakopoulos, A. R. Brown, A. Pomp, *J. Appl. Phys.* **1996**, *80*, 2501.
[43] I. P. M. Bouchoms, W. A. Schoonveld, J. Vrijmoeth, T. M. Klapwijk, *Synth. Met.* **1999**, *104*, 175.
[44] H. Yoshida, N. Sato, *Appl. Phys. Lett.* **2006**, *89*, 101919.
[45] M. Yoneya, M. Kawasaki, M. Ando, *J. Mater. Chem.* **2010**, *20*, 10397.
[46] R. A. Van Santen, *J. Phys. Chem.* **1984**, *88*, 5768.
[47] A. Brillante, I. Bilotti, R. G. Della Valle, E. Venuti, A. Girlando, M. Masino, F. Liscio, S. Milita, C. Albonetti, P. D'angelo, A. Shehu, F. Biscarini, *Phys. Rev. B* **2012**, *85*, 195308.
[48] A. Girlando, M. Masino, A. Brillante, T. Toccoli, S. Iannotta, *Crystals* **2016**, *6*, 41.
[49] L. Farina, A. Brillante, R. Della Valle, E. Venuti, M. Amboage, K. Syassen, *Chem. Phys. Lett.* **2003**, *375*, 490.
[50] S. Jena, D. Ray, *J. Phys. D: Appl. Phys.* **2020**, *54*, 015104.
[51] S. Verlaak, S. Steudel, P. Heremans, D. Janssen, M. S. Deleuze, *Phys. Rev. B* **2003**, *68*, 195409.
[52] A. Moser, J. Novák, H.-G. Flesch, T. Djuric, O. Werzer, A. Haase, R. Resel, *Appl. Phys. Lett.* **2011**, *99*, 221911.
[53] C. Westermeier, A. Cernescu, S. Amarie, C. Liewald, F. Keilmann, B. Nickel, *Nat. Commun.* **2014**, *5*, 4101.
[54] C. d. Dimitrakopoulos, P. r. l. Malenfant, *Adv. Mater.* **2002**, *14*, 99.
[55] N. Karl, *Synth. Met.* **2003**, *133–134*, 649.
[56] U. Sondermann, A. Kutoglu, H. Bassler, *J. Phys. Chem.* **1985**, *89*, 1735.
[57] E. Venuti, R. G. Della Valle, L. Farina, A. Brillante, M. Masino, A. Girlando, *Phys. Rev. B* **2004**, *70*, 104106.
[58] L. Pithan, D. Nabok, C. Cocchi, P. Beyer, G. Duva, J. Simbrunner, J. Rawle, C. Nicklin, P. Schäfer, C. Draxl, F. Schreiber, S. Kowarik, *J. Chem. Phys.* **2018**, *149*, 144701.
[59] R. K. Nahm, J. R. Engstrom, *J. Chem. Phys.* **2017**, *146*, 052815.
[60] S. R. Forrest, *Chem. Rev.* **1997**, *97*, 1793.
[61] D. R. T. Zahn, G. N. Gavrila, G. Salvan, *Chem. Rev.* **2007**, *107*, 1161.
[62] R. Schmidt, J. H. Oh, Y.-S. Sun, M. Deppisch, A.-M. Krause, K. Radacki, H. Braunschweig, M. Könemann, P. Erk, Z. Bao, F. Würthner, *J. Am. Chem. Soc.* **2009**, *131*, 6215.
[63] E. Kozma, M. Catellani, *Dyes Pigm.* **2013**, *98*, 160.
[64] A. J. Martínez-Galera, J. M. Gómez-Rodríguez, *J. Phys. Chem. C* **2019**, *123*, 1866.
[65] M. Möbus, N. Karl, T. Kobayashi, *J. Cryst. Growth* **1992**, *116*, 495.
[66] E. Hädicke, F. Graser, *Acta Cryst. C* **1986**, *42*, 189.
[67] K. Glöckler, C. Seidel, A. Soukopp, M. Sokolowski, E. Umbach, M. Böhringer, R. Berndt, W.-D. Schneider, *Surf. Sci.* **1998**, *405*, 1.
[68] B. Krause, A. C. Dürr, K. A. Ritley, F. Schreiber, H. Dosch, D. Smilgies, *Appl. Surf. Sci.* **2001**, *175–176*, 332.
[69] F. S. Tautz, *Prog. Surf. Sci.* **2007**, *82*, 479.
[70] C. Seidel, C. Awater, X. D. Liu, R. Ellerbrake, H. Fuchs, *Surf. Sci.* **1997**, *371*, 123.
[71] D. A. Tenne, S. Park, T. U. Kampen, A. Das, R. Scholz, D. R. T. Zahn, *Phys. Rev. B* **2000**, *61*, 14564.
[72] G. Salvan, D. A. Tenne, A. Das, T. U. Kampen, D. R. T. Zahn, *Org. Electron.* **2000**, *1*, 49.
[73] A. V. Dzyabchenko, V. E. Zavodnik, V. K. Belsky, *Acta Cryst. B* **1979**, *35*, 2250.
[74] H.-J. Nam, Y.-J. Kim, D.-Y. Jung, *Bull. Korean Chem. Soc.* **2010**, *31*, 2413.
[75] I. Salzmann, D. Nabok, M. Oehzelt, S. Duhm, A. Moser, G. Heimel, P. Puschnig, C. Ambrosch-Draxl, J. P. Rabe, N. Koch, *Cryst. Growth Des.* **2011**, *11*, 600.
[76] D. K. Hwang, K. Kim, J. H. Kim, S. Im, D.-Y. Jung, E. Kim, *Appl. Phys. Lett.* **2004**, *85*, 5568.
[77] G. Turrell, *Infrared and Raman Spectra of Crystals*, Academic Press, Cambridge, MA **1972**.
[78] Y. Sakamoto, T. Suzuki, M. Kobayashi, Y. Gao, Y. Fukai, Y. Inoue, F. Sato, S. Tokito, *J. Am. Chem. Soc.* **2004**, *126*, 8138.
[79] I. Salzmann, S. Duhm, G. Heimel, J. P. Rabe, N. Koch, M. Oehzelt, Y. Sakamoto, T. Suzuki, *Langmuir* **2008**, *24*, 7294.
[80] A. Brillante, I. Bilotti, R. G. Della Valle, E. Venuti, S. Milita, C. Dionigi, F. Borgatti, A. N. Lazar, F. Biscarini, M. Mas-Torrent, N. S. Oxtoby, N. Crivillers, J. Veciana, C. Rovira, M. Leufgen, G. Schmidt, L. W. Molenkamp, *CrystEngComm* **2008**, *10*, 1899.
[81] A. Tamayo, S. Riera-Galindo, A. O. F. Jones, R. Resel, M. Mas-Torrent, *Adv. Mater. Interfaces* **2019**, *6*, 1900950.
[82] R. P. Shibaeva, R. N. Lobkovskaya, V. N. Klyuev, *Cryst. Struct. Commun.* **1982**, *11*, 835.
[83] T. J. Emge, F. M. Wiygul, J. S. Chappell, A. N. Bloch, J. P. Ferraris, D. O. Cowan, T. J. Kistenmacher, *Mol. Cryst. Liq. Cryst.* **1982**, *87*, 137.
[84] M. Mamada, Y. Yamashita, *Acta Crystallogr., Sect. E: Struct. Rep. Online* **2009**, *65*, o2083.
[85] A. Brillante, I. Bilotti, R. G. Della Valle, E. Venuti, M. Mas-Torrent, C. Rovira, Y. Yamashita, *Chem. Phys. Lett.* **2012**, *523*, 74.
[86] B. Schrode, A. O. Jones, R. Resel, N. Bedoya, R. Schennach, Y. H. Geerts, C. Ruzié, M. Sferrazza, A. Brillante, T. Salzillo, E. Venuti, *Chem. Phys. Chem* **2018**, *19*, 993.
[87] A. O. F. Jones, Y. H. Geerts, J. Karpinska, A. R. Kennedy, R. Resel, C. Röthel, C. Ruzié, O. Werzer, M. Sferrazza, *ACS Appl. Mater. Interfaces* **2015**, *7*, 1868.
[88] N. Bedoya-Martínez, B. Schrode, A. O. Jones, T. Salzillo, C. Ruzié, N. Demitri, Y. H. Geerts, E. Venuti, R. G. Della Valle, E. Zojer, R. Resel, *J. Phys. Chem. Lett.* **2017**, *8*, 3690.
[89] T. Salzillo, A. Campos, A. Babuji, R. Santiago, S. T. Bromley, C. Ocal, E. Barrena, R. Jouclas, C. Ruzie, G. Schweicher, Y. H. Geerts, M. Mas-Torrent, *Adv. Funct. Mater.* **2020**, *30*, 2006115.
[90] M. Haisa, S. Kashino, R. Kawai, H. Maeda, *Acta Crystallogr. B* **1976**, *32*, 1283.
[91] T. N. Drebushchak, E. V. Boldyreva, *Z. Kristallogr. – Cryst. Mater.* **2004**, *219*, 506.
[92] M.-A. Perrin, M. A. Neumann, H. Elmaleh, L. Zaske, *Chem. Commun.* **2009**, *22*, 3181.

[93] H. M. A. Ehmann, O. Werzer, *Cryst. Growth Des.* **2014**, *14*, 3680.
[94] L. Pandolfi, A. Giunchi, A. Rivalta, S. D'Agostino, R. G. G. Della Valle, M. Mas-Torrent, M. Lanzi, E. Venuti, T. Salzillo, *J. Mater. Chem. C* **2021**, *9*, 10865.
[95] M. Irimia-Vladu, Eric. D. Głowacki, G. Voss, S. Bauer, N. S. Sariciftci, *Mater. Today* **2012**, *15*, 340.
[96] M. Irimia-Vladu, E. D. Głowacki, P. A. Troshin, G. Schwabegger, L. Leonat, D. K. Susarova, O. Krystal, M. Ullah, Y. Kanbur, M. A. Bodea, V. F. Razumov, H. Sitter, S. Bauer, N. S. Sariciftci, *Adv. Mater.* **2012**, *24*, 375.
[97] M. Irimia-Vladu, E. D. Głowacki, N. S. Sariciftci, S. Bauer, in *Small Organic Molecules on Surfaces: Fundamentals and Applications*, (Eds: H. Sitter, C. Draxl, M. Ramsey), Springer, Berlin, Heidelberg **2013**, p. 295.
[98] H. Von Eller, *Bull.Soc.Chim.Fr* **1955**, *106*, 1433.
[99] W. Haase-Wessel, M. Ohmasa, P. Susse, *Naturwissenschaften* **1977**, *64*, 435.
[100] F. G. del Pozo, S. Fabiano, R. Pfattner, S. Georgakopoulos, S. Galindo, X. Liu, S. Braun, M. Fahlman, J. Veciana, C. Rovira, X. Crispin, M. Berggren, M. Mas-Torrent, *Adv. Funct. Mater.* **2016**, *26*, 2379.
[101] B. Servet, G. Horowitz, S. Ries, O. Lagorsse, P. Alnot, A. Yassar, F. Deloffre, P. Srivastava, R. Hajlaoui, *Chem. Mater.* **1994**, *6*, 1809.
[102] L. Pithan, C. Cocchi, H. Zschiesche, C. Weber, A. Zykov, S. Bommel, S. J. Leake, P. Schäfer, C. Draxl, S. Kowarik, *Cryst. Growth Des.* **2015**, *15*, 1319.
[103] G. Horowitz, B. Bachet, A. Yassar, P. Lang, F. Demanze, J.-L. Fave, F. Garnier, *Chem. Mater.* **1995**, *7*, 1337.
[104] T. Siegrist, R. M. Fleming, R. C. Haddon, R. A. Laudise, A. J. Lovinger, H. E. Katz, P. Bridenbaugh, D. D. Davis, *J. Mater. Res.* **1995**, *10*, 2170.
[105] A. Brillante, I. Bilotti, C. Albonetti, J.-F. Moulin, P. Stoliar, F. Biscarini, D. M. de Leeuw, *Adv. Funct. Mater.* **2007**, *17*, 3119.
[106] J.-F. Moulin, F. Dinelli, M. Massi, C. Albonetti, R. Kshirsagar, F. Biscarini, *Nucl. Instrum. Methods Phys. Res., Sect. B* **2006**, *246*, 122.
[107] A. Moser, I. Salzmann, M. Oehzelt, A. Neuhold, H.-G. Flesch, J. Ivanco, S. Pop, T. Toader, D. R. T. Zahn, D.-M. Smilgies, R. Resel, *Chem. Phys. Lett.* **2013**, *574*, 51.
[108] T. Salzillo, A. Girlando, A. Brillante, *J. Phys. Chem. C* **2021**, *125*, 7384.
[109] A. Otto, in *Light Scattering in Solids IV: Electronics Scattering, Spin Effects, SERS, and Morphic Effects*, (Eds: M. Cardona, G. Güntherodt), Springer, Berlin, Heidelberg **1984**, p. 289.
[110] R. Pilot, R. Signorini, C. Durante, L. Orian, M. Bhamidipati, L. Fabris, *Biosensors* **2019**, *9*, 57.
[111] J. Langer, D. Jimenez de Aberasturi, J. Aizpurua, R. A. Alvarez-Puebla, B. Auguié, J. J. Baumberg, G. C. Bazan, S. E. J. Bell, A. Boisen, A. G. Brolo, J. Choo, D. Cialla-May, V. Deckert, L. Fabris, K. Faulds, F. J. García de Abajo, R. Goodacre, D. Graham, A. J. Haes, C. L. Haynes, C. Huck, T. Itoh, M. Käll, J. Kneipp, N. A. Kotov, H. Kuang, E. C. Le Ru, H. K. Lee, J.-F. Li, X. Y. Ling, et al., *ACS Nano* **2020**, *14*, 28.
[112] H. Baessler, G. Vaubel, *Phys. Rev. Lett.* **1968**, *21*, 615.
[113] H. Baessler, H. Killesreiter, G. Vaubel, *Discuss. Faraday Soc.* **1971**, *51*, 48.
[114] G. Vaubel, H. Baessler, D. Möbius, *Chem. Phys. Lett.* **1971**, *10*, 334.
[115] P. Li, Z.-H. Lu, *Small Sci.* **2021**, *1*, 2000015.
[116] T. Muck, V. Wagner, U. Bass, M. Leufgen, J. Geurts, L. W. Molenkamp, *Synth. Met.* **2004**, *146*, 317.
[117] X.-Y. Zhu, *J. Phys. Chem. B* **2004**, *108*, 8778.
[118] F. Biscarini, R. Zamboni, P. Samorí, P. Ostoja, C. Taliani, *Phys. Rev. B* **1995**, *52*, 14868.
[119] Y. Cho, J. Huang, C. W. Wong, *Appl. Phys. Lett.* **2020**, *116*, 020501.
[120] W. Han, P. Huang, L. Li, F. Wang, P. Luo, K. Liu, X. Zhou, H. Li, X. Zhang, Y. Cui, T. Zhai, *Nat. Commun.* **2019**, *10*, 4728.
[121] A. H. Castro Neto, F. Guinea, N. M. R. Peres, K. S. Novoselov, A. K. Geim, *Rev. Mod. Phys.* **2009**, *81*, 109.
[122] A. B. Cairns, A. L. Goodwin, *Chem. Soc. Rev.* **2013**, *42*, 4881.
[123] T. R. Welberry, B. D. Butler, *Chem. Rev.* **1995**, *95*, 2369.

Tommaso Salzillo is Assistant Professor at University of Bologna. He graduated in Industrial Chemistry in 2011 and he received his Ph.D. in physical chemistry in 2015 from the University of Bologna. He was Marie Curie Postdoctoral Fellowship in 2017 at ICMAB-CSIC (Spain) studying the polymorphism and morphology control in flexible organic electronic devices. From 2020 he was Senior Postdoc at Weizmann Institute of Science (Israel) performing studies on the structural dynamics of functional materials such as organic crystal and chalcogenide perovskites by means of low-wavenumber Raman spectroscopy. His research interests include polymorphism in molecular materials, solid-state photoreactions and vibrational spectroscopy.

Aldo Brillante is a retired professor in Physical Chemistry at Bologna University. He graduated at the University of Bologna, was a former postgraduate student of D.P. Craig (Australian National University) and was appointed in the midseventies by IBM Research Laboratories (San Jose) as postdoctoral fellow in a surface science project. He spent several periods at the University of Düsseldorf (surface plasmons) and at the MPI FkF Stuttgart (high pressure spectroscopy). His activity has been mostly dedicated to the study of elementary excitations in solids (excitons, phonons, plasmons and polaritons). He is currently studying polymorphism, crystal-to-crystal photoreactions and lattice phonons.